Molecular Crystals and Liquid Crystals Science and Technology. Section A. Molecular Crystals and Liquid Crystals

Publication details, including instructions for authors and subscription information:
http://www.tandfonline.com/loi/gmcl19

Homogeneous Optical Properties of Semiconductor Nanocrystals

U. Banin [a], A. Mews [a], A. V. Kadavanich [a], A. A. Guzelian [a] & A. P. Alivisatos [a]

[a] Department of Chemistry, University of California at Berkeley, Berkeley, CA, 94720

Version of record first published: 24 Sep 2006.

To cite this article: U. Banin, A. Mews, A. V. Kadavanich, A. A. Guzelian & A. P. Alivisatos (1996): Homogeneous Optical Properties of Semiconductor Nanocrystals, Molecular Crystals and Liquid Crystals Science and Technology. Section A. Molecular Crystals and Liquid Crystals, 283:1, 1-10

To link to this article: http://dx.doi.org/10.1080/10587259608037856

Mol. Cryst. Liq. Cryst., 1996, Vol. 283, pp. 1–10
Reprints available directly from the publisher
Photocopying permitted by license only

HOMOGENEOUS OPTICAL PROPERTIES OF SEMICONDUCTOR NANOCRYSTALS

U. BANIN, A. MEWS, A. V. KADAVANICH, A. A. GUZELIAN, and A. P. ALIVISATOS
Department of Chemistry, University of California at Berkeley, Berkeley CA 94720

Abstract In between the molecular and bulk forms of matter, semiconductor nanocrystals are novel materials with interesting optical and electronic properties. We present a study of the homogeneous optical properties of two nanocrystal systems. First, the homogeneous absorption of InP nanocrystals is studied via hole burning experiments. The optical spectrum consists of a HOMO-LUMO transition with a 10 meV width and a second electronic transition shifted by 0.11 eV. The optical transitions are assigned within a three valence-band model.

The CdS/HgS/CdS quantum-dot/quantum-well system is also investigated and a transmission electron microscopy study shows that the growth of the HgS well region and the CdS outer layer is epitaxial. Selective optical techniques are used to study the electronic level structure. In hole burning, a discrete transition (width of 7 meV) with pronounced phonon side bands at a frequency of 250 cm^{-1} is observed. In fluorescence, the line narrowed spectrum also shows phonon replicas at a similar frequency. The measurements provide direct evidence for charge localization in the low band gap HgS well region within this colloidally synthesized nano-heterostructure.

1. INTRODUCTION

Semiconductor nanocrystals of diameters in the range of 10-100 Å lie in between the molecular and solid state forms of matter.[1] The ability to control the size of the crystallites allows a study of the evolution of various optical, electronic and structural properties in this size regime. Such control may prove useful in various applications of these materials as building blocks in optical or electro-optical devices.[2]

Typically, a semiconductor nanocrystal consists of hundreds to thousands of atoms with a crystal structure similar to that of the bulk semiconductor material. The nanocrystals are prepared via a 'ground up' approach using wet chemical synthesis and are often referred to as a new class of large molecules.[3] The nanocrystal surface is capped with organic moieties which prevent aggregation, confer solubility in various solvents and should also provide electronic passivation by eliminating surface dangling orbitals. Due to their molecular nature, a whole arsenal of chemical techniques can be used to manipulate nanocrystals. They may be dissolved in a fluid, blended into a polymer or attached to an electrical circuit for potential applications. It is also possible to form

nanocrystal assemblies of various kinds, such as arrays or three dimensional crystals.[4,5] Thus nanocrystals prepared by wet chemical techniques may serve as building blocks for more complex structures which cannot be prepared by traditional lithographic techniques.

The materials that we study are in the strong quantum confinement regime in which the particle radius is smaller then the bulk exciton Bohr radius. Early theoretical predictions for three dimensional quantum confined semiconductors in this regime suggested that the discretization of states will ultimately lead to concentration of enormous oscillator strength into a single molecular like discrete transition in a quantum dot.[6] Combined with the high polarizibility of charge in such a particle, one should expect large χ_3 values leading to interesting non-linear optical properties. However, broadening of the homogeneous linewidth will dilute the oscillator strength and limit the magnitude of the predicted enhancement. The homogeneous linewidth[7] and the detailed optical level structure in these materials is of considerable importance for this issue.

In this paper, we review our recent photophysical studies of two different nanocrystal systems - first we present a study of the homogeneous optical properties of a III-V semiconductor material in the strong confinement regime - namely InP. From the point of view of optical and photophysical properties, the study of III-V nanocrystal systems is particularly interesting in connection with the ability to conduct a comparative investigation of the behavior with that of the prototypical II-VI CdSe system. The different ionic character, effective masses and band structure renders such a study valuable for checking and studying quantum confinement effects and the validity of theoretical models.

This is followed by a study on the quantum-dot quantum well (QDQW) CdS/HgS/CdS nano-heterostructure system in which the low band gap HgS layer forms an inner well region for charge carrier localization.[8] In this system, surface passivation is achieved by inorganic capping of a low band gap material by an epitaxially grown layer of a high band gap material. The realization and effects of this approach and the resultant spectral features which provide evidence for charge localization in the well region will be discussed.

2. HOMOGENEOUS OPTICAL PROPERTIES OF InP NANOCRYSTALS:

Recent advances in synthesis have led to the production of crystalline, soluble and monodisperse samples of InP.[9,10] While nanocrystals of II-VI materials such as CdS and CdSe have been studied extensively, the progress in the investigation of III-V materials has lagged because of difficulties in the synthesis. In the II-VI case, the bare atoms or ions can be used as precursors thus enabling direct reaction of the relevant elements and

enabling the control and separation of the nucleation and growth steps. Due to the more covalent character of III-V materials atomic or ionic precursors can not be used. Thus the use of organometallic precursors is implemented and this results in the presence of large reaction barriers complicating the desired nucleation and growth sequence. Very recently, Nozik and co-workers have reported a successful synthesis route to produce crystalline and soluble InP nanocrystals.[9] We have modified their synthesis and employed the tools of surface modification and size selective precipitation with the goal of controlling nanocrystal size distributions and surface passivation.[10] For low temperature photophysical studies the particles were embedded in thin PVB (poly-vinyl-butyral) polymer films.

As these particles still have a size distribution of +/- 20%, we have employed size selective optical techniques to study the homogeneous optical properties of this sample. Transient nanosecond hole burning (HB) allows the 'single particle' absorption spectra to be obtained.[11] The principle of this technique is that via optical excitation with a narrow laser pulse a small subset of the ensemble is selectively excited. The ensuing spectral bleach (spectral hole) probed at a delay of several nsec, contains information about the absorption of this subset.

In Figure 1a, the low temperature absorption spectrum of InP nanocrystals with a mean diameter of 34 Å is presented. The band gap is shifted from the bulk by approximately 0.5 eV as a result of quantum confinement. Aside from an excitonic feature apparent as a shoulder at ~1.9 eV, no additional structure is observed. In Figure 1b, the transient hole spectrum for this sample, measured at three different excitation frequencies is displayed. In each case, a narrow bleach feature centered at the pump frequency is observed, riding on a substantially broader background. The pump wavelength dependence of the hole spectrum is as expected for an inhomogeneously broadened sample; Upon excitation at the absorption edge (a_1), only the largest nanocrystals in the ensemble are excited. The narrow feature at the excitation wavelength in the hole spectrum (b_1), results from bleaching of the HOMO-LUMO transition, whereas the shoulder at ~310 cm^{-1} is assigned to a phonon sideband. In a molecular picture, the sideband reflects the bleached absorption to high vibrational levels in the first excited electronic state of the nanocrystal. The broad feature spaced by ~0.1 eV, can be explained as bleaching of the absorption to a second electronic transition. The bleach spectrum in this case is closely related to the single particle absorption spectra. As the excitation is tuned to the blue of the inhomogeneous absorption (a_2, a_3), the homogeneous spectrum of particles excited in their HOMO-LUMO transition, is riding on a broad background (b_2, b_3). This background results from the bleach spectrum of other particles excited into their higher transitions. Unlike typical molecular hole burning

spectra, which contain usually an inhomogeneously broadened single transition, the semiconductor nanocrystal optical spectra is composed of a sequence of nearly overlapping discrete states, yielding the observed hole burning spectral pattern.

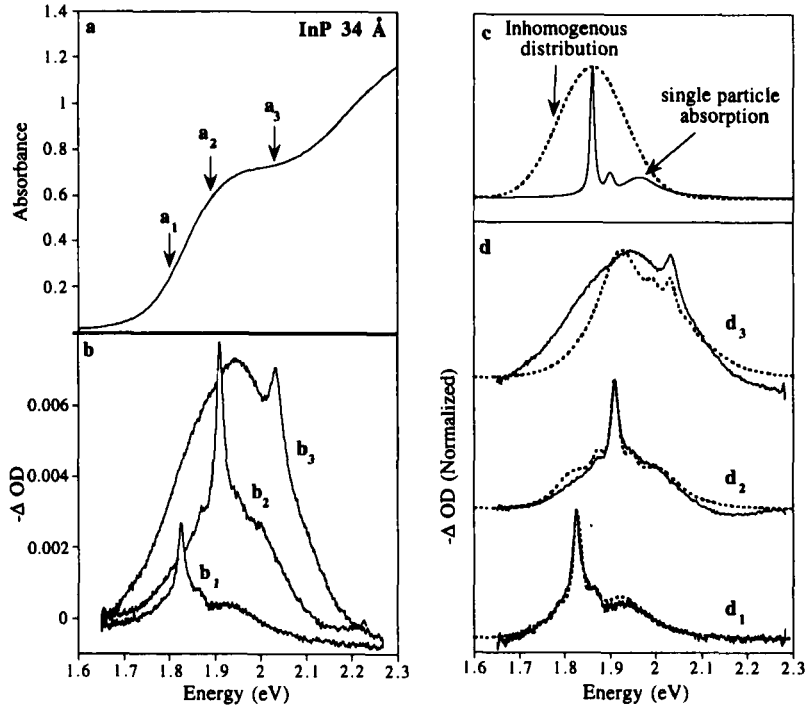

FIGURE 1. Hole burning spectra for InP nanocrystals with a mean diameter of 34 Å at T=6K. The absorption spectrum is shown in frame a, the arrows depict the pump laser energies for the hole burning spectra presented in frame b. In frame c, the model single particle absorption spectra (solid line) consisting of a narrow HOMO-LUMO transition along with a phonon side band and a second electronic transition at a spacing of 0.11 eV is shown. In frame d, the results of the simulated holes (dotted lines), are compared with the normalized experimental spectra (solid lines).

The HB spectrum can be simulated in order to extract the single particle absorption spectra.[11,12] The results of such a simulation for the 34 Å InP particles are presented in Figure 1d, along with the calculated inhomogeneous linewidth and single particle absorption spectra (Figure 1c). The model for the single particle absorption consists of a narrow (10 meV) HOMO-LUMO transition along with a phonon sideband at a spacing of 310 cm^{-1} which resembles the frequency of bulk InP optical phonons.[13] A second -

excited state transition separated by 0.11 eV which is considerably broadened (full width at half maximum of 100 meV) is also included. These optical transitions in InP nanocrystals may be assigned to a transfer of an electron from the mostly phosphorous *3p* like valence band levels to the In *5s* conduction band levels. The observed optically active transitions arise from the splitting of the valence band electronic structure in the regular three band model consisting of a light hole and heavy hole bands degenerate at Γ, and the third spin- orbit split off band. To a first approximation, the first transition occurs then between the light and heavy hole bands and the valence band, and the second observed transition is from the split off band (the Δ parameter for the splitting of the split off band in the bulk is 0.11 eV).[13] Mixing among these levels at finite size however, may lead to appearance of various hole band levels which could be modeled within a particle in a spherical box picture.[14] A detailed study with a theoretical model will be presented elsewhere.

The linewidth of the InP nanocrystals is slightly smaller then that observed for similar sized CdSe nanocrystals. The organically passivated systems of InP and CdSe seem to exhibit similar behavior. As inelastic scattering or trapping at the surface may be a contributing factor to the linewidth[7] it is of interest to examine different approaches to surface passivation. One possibility is the inorganic 'capping' of the interior by growth of a higher gap semiconductor material to minimize surface effects. A system in which such an approach is attempted is the subject of the next section.

2. HOMOGENEOUS OPTICAL PROPERTIES OF CdS/HgS/CdS NANO-QUANTUM-WELLS:

Chemical synthesis of single material nanocrystals has been demonstrated for a variety of semiconductor systems. An additional challenge is presented in the quest to selectively engineer heterostructured materials in what would be considered as the chemical counterpart for lithography techniques. Recently, Weller and coworkers have developed such a nanocrystalline heterostructure in which HgS, a low bandgap material, is embedded as a spherical shell within a CdS quantum dot.[8] In such a structure, charge carriers are expected to localize in the quantum well region formed by the HgS layer. Previously this structure was characterized by chemical methods and the proposed charge carrier localization was based upon the observed shifts in the optical spectra.[15] In this work we show that we have direct evidence for an epitaxial growth of the different layers and that the charge carrier excitation and recombination does indeed occur in the HgS region of the particles.

The preparation of the quantum-dot/quantum-well particles, has been described in detail elsewhere[8] and a summary of the synthesis is presented in figure 2. The first step is the formation of the CdS core which is performed by a reaction of a dissolved cadmium salt with H_2S in the presence of hexametaphosphate (HMP) acting as a polar surfactant. The pH of the solution is used to control and separate the nucleation and growth steps, a necessary condition for achieving monodispersity. The reaction is initiated at a basic pH, which favors rapid nucleation of CdS crystallites. In this process the H_2S is depleted and protons are released. Thus the pH quickly drops below the threshold for nucleation and the reaction proceeds under conditions favoring slow growth.

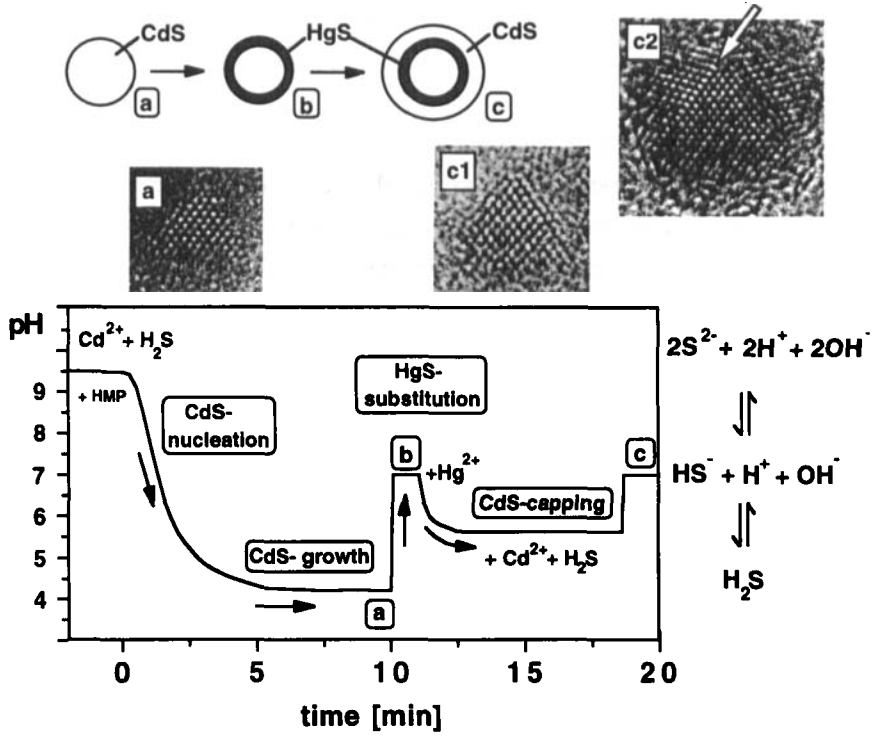

FIGURE 2. Schematic synthesis route for the formation of the CdS/HgS/CdS QDQW system. The pH of the solution is used to control the nucleation and growth steps. The HRTEM pictures for the core particles (a) reveal that they have a tetrahedral shape, which is maintained upon the growth of the HgS well layer (b). The final growth stage of the outer CdS cap (c), leads to two different morphologies. A tetrahedral shape which represents homogenous growth (c1), and a second shape (c2), in which a stacking fault appears leading to a crystallographic mismatch of the cap. In this case, the CdS tetrahedral core is clearly resolvable, and the HgS region shows enhanced contrast (arrow). All growth stages are epitaxial. See text for details.

High Resolution Electron Microscopy (HRTEM) reveals that the CdS core particles formed in this first step are not spherical but show a tetrahedral shape (Figure 2a). This can be explained by assuming that the nanocrystals which form a cubic zincblende lattice structure are exposing stable 111 surfaces. Taking into account the fact that the HMP surface ligands are negatively charged, this is consistent with cadmium rich 111 surfaces for the core particles. As the size of these particles is comparable to the bulk CdS exciton diameter (50 Å), the absorption spectra presented in figure 3a exhibits only a small shift from the bulk band gap of 2.5 eV.

In the next step of the preparation, the surface cadmium ions are exchanged with Mercury. The tetrahedral morphology is preserved in this step (Figure 2b), and the absorption spectrum exhibits a shift to the red of the bulk CdS gap. The final coating of the particles is carried out by adding excess cadmium ions to the solution and growing CdS on top of the HgS layer via slow H_2S injection at pH of 5.5, suppressing the nucleation of new CdS particles. The final CdS capping leads to a further red shift of the absorption onset to ~2 eV (Figure 3c). Such a red shift below the bulk band gap of the CdS cap, only occurs in systems of low dimensionality, where the increased size reduces the effect of quantum confinement. In addition, at this stage substantial luminescence with a yield of several percent is observed (Figure 3). This is a direct result of the surface passivation provided by the outermost CdS cap that eliminates nonradiative surface traps from the HgS layer recombination region.

The structural analysis (Figure 2c) reveals that ~60% of the particles exhibit tetrahedral shape with an edge length of 60 Å reflecting homogeneous growth of the particles (Figure 2, c1). In addition, no amorphous region can be seen suggesting epitaxial growth is taking place. Half of the non-tetrahedral particles show a different shape (Figure 2, c2) where the CdS caps are crystallographicaly mismatched to the cores. This can be explained by the appearance of one hexagonal stacking fault at the interface of the HgS and CdS layers. In this particle the initial tetrahedral core can clearly be resolved and the enhanced contrast at the interface (c2, arrow) may result from the HgS layer. Detailed structural work along with computer simulations are in progress.

While the complete heterostructure exhibits spectral features at the expected energy and also displays substantial enhancement of the luminescence quantum yield, the spectra lack the discrete structure required by quantum confinement. As in the InP case, this calls for the use of size selective optical techniques in order to obtain the homogeneous optical spectra. The low temperature (T = 6 K) hole burning spectrum for CdS/HgS/CdS is shown in Figure 3. It reveals that very large inhomogeneous broadening is present in the sample. At the excitation frequency, a narrow hole from which we extract a homogeneous width of 55 cm^{-1} (7 meV) is observed. In addition, distinct phonon side

bands appear at a spacing of 250 cm^{-1} (see inset of Figure 3). The appearance of the sidebands reflects the strong coupling of the electronic excitation to LO phonons, which results from the distortion of the ionic lattice upon the alteration of the charge distribution in the sample.[16] This coupling is stronger in the more ionic II-VI nanocrystals as compared with InP, a III-V material which is more covalent.

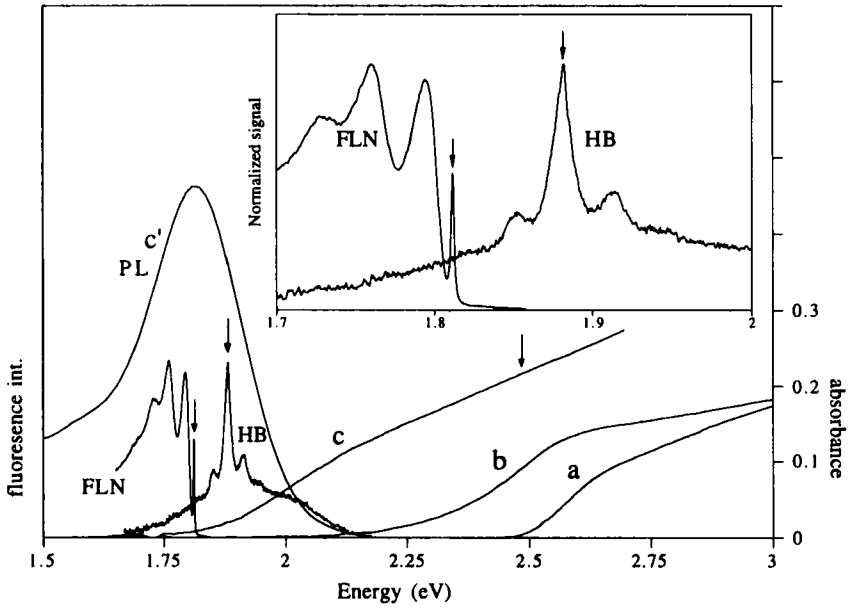

FIGURE 3. Inhomogeneous and homogeneous optical spectra for the CdS/HgS/CdS system. The inhomogeneous spectra are presented along with the results of the FLN and HB experiments. The HgS covered particles (b), exhibit a red shift relative to the CdS core particles (a). The absorption (c) and emission spectra (c') of the final CdS/HgS/CdS particles is also shown. Representative HB and FLN spectra show the underlying spectral features. In the insert the FLN and HB are enlarged, and the phonon structure on them is clearly apparent. Arrows indicate the position of the pump laser for the various experiments. The narrow peak at the excitation frequency in the FLN trace, is residual laser scatter used to mark the excitation position.

Several features of the spectra provide evidence for localization of charge in the low band gap HgS well region. The isolated transition with the narrow linewidth observed in the HB experiment, shows the existence of a strongly allowed discrete transition at the particle band gap. Such molecular like discretization is expected to appear within the strongly confined, single monolayer HgS well region. Examination of the LO phonon frequency observed in the HB spectra, yields further evidence for this conclusion. The

CdS bulk LO phonon frequency is 300 cm^{-1} while the frequency of bulk HgS LO mode is 253 cm^{-1}.[16,17] The frequency observed in the experiment is equal to the HgS LO frequency despite the fact that the Hg cation fraction is only 20%. This is consistent with a picture of localized excitation in the thin HgS layer, leading to coupling mostly to an HgS-like LO mode.

Further evidence for the charge localization in the HgS well region is provided by fluorescence line narrowing (FLN) measurements. FLN achieves optical selection by excitation on the red edge of the absorption spectrum where only a small subset of the ensemble of nanocrystals absorbs.[18] The luminescence is then detected a few nanoseconds later with a gated multi channel detector to minimize scattered light from the pump laser. In this case, instead of a broad structureless emission peak, the underlying emission exhibits a progression in an LO phonon mode. We extract a 255 cm^{-1} LO mode for the first two peaks, which varies to slightly lower frequencies for the higher vibrational levels. Adopting again a molecular view, the phonon progression observed in the FLN reflects the 'ground state' vibrational spacing as emission takes place from the relaxed excited state, to several vibrational levels of the ground state. The observation suggests that not only the absorption, but also the radiative recombination of electrons and holes takes place centered in the HgS well region. A more detailed understanding of the charge localization in the CdS/HgS/CdS system awaits additional study of the phonon structure and theoretical calculations of the electron-phonon coupling.

An additional interesting feature of the FLN spectra is the appearance of a 150 cm^{-1} (19 meV) shift between the excitation frequency and the first emission peak position. This can be explained only by assuming that the emitting state is different from the absorbing state. This kind of behavior has been previously reported for CdSe nanocrystals,[18] and the nature of the emitting state in nanocrystals is a subject of current debate.

4. CONCLUSIONS

Quantum confinement effects in two nanocrystalline systems have been studied via selective optical techniques. The study of InP nanocrystals reveals that the electronic structure consists of a HOMO-LUMO transition with a second transition at 0.11 eV from the gap. The homogeneous linewidth is comparable to that observed in similar sized CdSe.

The study of the CdS/HgS/CdS quantum-dot in a quantum well system showed that epitaxial growth leads to formation of an HgS well region. The optical studies provide

conclusive evidence that the charge carriers indeed localize in this layer. The large inhomogeneous broadening arises as a result of size and morphology variations.

The linewidth issue in nanocrystals has yet to be resolved. How much of this is an intrinsic size effect remains an open question currently under study. However, chemical manipulation and synthesis provides powerful means for tailoring the optical properties of complex quantum dot systems.

REFERENCES

1. L. E. Brus, Appl. Phys. A 53, 465 (1991).
2. V. L. Colvin, M. C. Schlamp, and A. P. Alivisatos, Nature 370, 354 (1994).
3. M. L. Steigerwald, and L. E. Brus, Acc. Chem. Res. 23, 183 (1990).
4. N. Herron, J. C. Calabrese, W. E. Farneth, and Y. Wang, Science 259, 1426. (1993).
5. C. B. Murray, C. R. Kagan, and M. G. Bawendi, Science 270, 1335 (1995).
6. S. Schmitt-Rink, D. A. B. Miller, and D. S. Chemla, Phys. Rev. B 35, 8113 (1987).
7. D. M. Mittleman, R. W. Schoenlein, J. J. Shiang, V. L. Colvin, A. P. Alivisatos, and C. V. Shank, Phys. Rev. B 49, 14435 (1994).
8. A. Mews, A. Eychmüller, M. Giersig, D. Schooss, and H. Weller, J. Phys. Chem 98, 934 (1994).
9. O. I. Micic, C. J. Curtis, K. M. Jones, J. R. Sprague, and A. J. Nozik, J. Phys. Chem. 98, 4966 (1994); O. I. Micic, J. R. Sprague, C. J. Curtis, K. M. Jones, J. L. Machol, A. J. Nozik, B. Giessen, B. Fluegel, G. Mohs, N. Peyghambarian, J. Phys. Chem. 99, 7754 (1995).
10. A. A. Guzelian, J. E. B. Katari, A. V. Kadavanich, U. Banin, K. Hamad, E. Juban, and A. P. Alivisatos, R. H. Wolters, C. C. Arnold, and J. R. Heath, JACS, submitted for publication.
11. A. P. Alivisatos, A. L. Harris, N. J. Levinos, M. L. Steigerwald and L. E. Brus, J. Chem. Phys. 89, 4001 (1988).
12. D. J. Norris, and M. G. Bawendi, J. Chem. Phys. 103, 5260 (1995).
13. Landolt-Bornstein, New Series, K. H. Hellwege editor in chief, Group III Vol. 17a, pp 281-297, Springer-Verlag, Berlin (1982).
14 A. I. Ekimov, F. Hache, M. C. Schanne-Klein, D. Ricard, C. Flytzanis, I. A. Kudryavtsev, T. V. Yazeva, A. V. Rodina, and A. L. Efros, J. Opt. Soc. Am. B 10, 100 (1993).
15. D. Schooss, A. Mews, A. Eychmüller, H. Weller, Phys. Rev. B 49, 17072 (1994).
16. J. J. Shiang, S. H. Risbud, A. P. Alivisatos, J. Chem. Phys. 98, 8432 (1993).
17. W. Szuszkiewicz, B. Witkowska, M. Jouanne, Acta Phys. Pol. A 87, 415 (1995).
18. M. Nirmal, C. B. Murray, M. G. Bawendi, Phys. Rev. B 50, 2293 (1994).